Silver nanoparticles coupled to anti-EGFR antibodies sensitize nasopharyngeal carcinoma cells to irradiation

DAHAI YU[1,2*], YAN ZHANG[3*], HONG LU[1,2] and DI ZHAO[1,2]

[1]Jiangsu Collaborative Innovation Center of Tumor Prevention and Treatment by Traditional Chinese Medicine (TCM), Nanjing University of Chinese Medicine, Nanjing, Jiangsu 210023; [2]Department of Radiotherapy, Jiangsu Province Hospital of Traditional Chinese Medicine, Affiliated Hospital of Nanjing University of Traditional Chinese Medicine; [3]Department of Clinical Laboratory, Jiangsu Province Hospital, The First Affiliated Hospital of Nanjing Medical University, Nanjing, Jiangsu 210029, P.R. China

Received July 29, 2016; Accepted July 24, 2017

DOI: 10.3892/mmr.2017.7704

Abstract. Radiotherapy is the major form of treatment for head and neck carcinoma, a malignant tumour of epithelial origin. The identification of agents, which can be co-administered in order to sensitize these tumours to radiotherapy, has become a major focus of investigations. In the present study, a novel 20 nm nanocomposite, Ag/C225, was constructed, which consisted of silver nanoparticles (AgNPs) conjugated to an epidermal growth factor receptor-specific antibody (C225). Physical characterization demonstrated that the Ag/C225 nanoparticles were spherical and dispersed well in water. Enzyme-linked immunosorbent assays showed that the activity of C225 was preserved in the Ag/C225 nanoparticles. The results of 3-(4,5-dimethylthiazol-2-yl)-2,5-diphenyltetrazolium bromide analysis revealed that AgNPs and Ag/C225 inhibited the proliferation of nasopharyngeal carcinoma epithelial (CNE) cells in a dose- and time-dependent manner. Flow cytometry revealed that AgNPs and Ag/C225 induced the apoptosis of CNEs, and abrogated G2 arrest; the latter effect was more marked with Ag/C225 than with AgNPs. Clonogenic assays indicated that AgNPs and Ag/C225 increased the sensitivity of CNEs to irradiation. The sensitizer enhancement ratios were 1.610±0.012 and 1.405±0.033 Gy for AgNPs and Ag/C225, respectively. Western blot analysis revealed that combining X-ray irradiation with either AgNPs or Ag/C225 reduced the expression levels of DNA damage/repair proteins Ku-70, Ku-80 and Rad51; Ag/C225 was also more effective than AgNPs in this context. These results indicated that AgNPs and Ag/C225 effectively enhanced CNE cell radiosensitivity *in vitro*. Therefore, these potent agents may be considered for use as radiosensitizers during the treatment of human nasopharyngeal carcinoma.

Correspondence to: Dr Di Zhao, Department of Radiotherapy, Jiangsu Province Hospital of Traditional Chinese Medicine, Affiliated Hospital of Nanjing University of Traditional Chinese Medicine, 155 Hanzhong Road, Nanjing, Jiangsu 210029, P.R. China
E-mail: 9964307@qq.com

Dr Yan Zhang, Department of Clinical Laboratory, Jiangsu Province Hospital, The First Affiliated Hospital of Nanjing Medical University, 300 Guangzhou Road, Nanjing, Jiangsu 210029, P.R. China
E-mail: 67658837@qq.com

*Contributed equally

Key words: radiotherapy, radiosensitivity, molecular targeted therapy, nasopharyngeal carcinoma cells

Introduction

Nanotechnology is increasingly used in the biomedical field, as the materials generated have notable physicochemical properties on the nanometer scale (1-3). Advances in nanotechnology, and our understanding of cellular and molecular biology have provided various biomedical imaging modalities and nanosized imaging agents (4). The surface of nanomaterials is important in crossing the cell membrane: Nano-cores and functional molecules are often incorporated to enhance cellular penetration (5-7). In order to improve anticancer therapeutic effects, nanosized particulate systems based on the merging of nanotechnology with modern biology techniques have been created (4,8).

Radiotherapy is a major treatment modality for malignant tumours, particularly in the case of nasopharyngeal carcinoma, which originates from the epithelium and is one of the most common malignant tumours in southern China (9). Nasopharyngeal carcinoma is particularly radiosensitive; therefore radiotherapy has been a principal front line treatment. However, this approach has certain limitations; in order to avoid toxicity to healthy tissues, a high single irradiation dose is fractionated into several lower dose treatments. Unfortunately, this strategy fails during the later stages of treatment, as the rate of tumour cell proliferation increases and outpaces the cytotoxic effects of irradiation (10). Therefore, an aim of current investigations in the field is to identify additional agents, which can act as radiosensitizers.

The advent of targeted cancer therapies has led to the development of potent tumour-specific agents, which show reduced toxicity towards normal tissues. Epidermal growth

factor receptor (EGFR) is the member of a family of four ErbB receptor tyrosine kinases. The activation of EGFR triggers the phosphatidylinositol 3-kinase (PI3K)/Akt pathway (11). In several human malignancies, including colorectal cancer and non-small cell lung cancer, the overexpression of EGFR correlates with tumour cell growth, altered cell metabolism, and increased proliferation and angiogenesis; these perturbations lead to disease progression, including local invasion and metastasis (12). In previous years, several inhibitors have been developed, which are designed to treat malignant tumours by disrupting PI3 K/Akt signalling cascades and preventing the development of metastasis (13). Different approaches have been used to target EGFR, including the use of small molecules, including gefitinib (Iressa) or lapatinib (Tyverb), and humanized monoclonal antibodies targeting EGFR, including cetuximab (Erbitux; C225). C225 can exert effective locoregional control of tumour growth and reduce mortality rates, without increasing the common toxic effects associated with radiotherapy to the head and neck (14-16). However, resistance to these drugs, possibly due to the build-up of hypoxia in solid tumours, invariably develops. Hypoxic tumours are characterized by more aggressive and metastatic phenotypes, with lower sensitivity to treatments, and are associated with a poor prognosis.

In our previous study, silver (Ag)-based nanoparticles (AgNPs) were found to have potential utility as radiosensitizers. For example, AgNPs with diameters of 20-50 nm significantly sensitize glioma cells to irradiation, and this radiosensitization effect of AgNPs has important implications in the design of nanotechnology-based radiosensitizers to improve the outcomes of cancer radiotherapy (17). Therefore, in the present study, AgNPs coupled to C225 were designed, and their use in radiotherapy was evaluated. The Ag/C225 conjugates significantly inhibited the growth of CNEs in a dose- and time-dependent manner. Ag/C225 enhanced the suppression of clonogenic cell growth, which was induced by X-ray irradiation. The potency of the Ag/C225 and X-ray combination was attributed, at least in part, to the suppression of EGFR signalling. Therefore, Ag/C225 offers potential as either a radiosensitizer or targeted radiotracer in clinical radiotherapy.

Materials and methods

Preparation of AgNPs and Ag/C225 nanocomposites. The AgNP colloid was prepared by thermal reduction of 10 mM $AgNO_3$ aqueous solution in the presence of 15 mM trisodium citrate at 90˚C. Subsequent to the solution turning green within 30 sec; it was rapidly cooled in an ice bath. The citrate ions act as reductants and stabilizers of Ag particles in solution. The synthesized sol-1 (20 ml) was reacted with 0.2 ml of 0.1 mM hexadecyl trimethyl ammonium bromide (CTAB) aqueous solution at room temperature for 15 min, in order to prevent the excess aggregation of CTAB-modified Ag colloids. The AgNPs were self-assembled on poly (diallyldimethylammonium chloride (PDDA)-modified (1% w/w) glass slides by immersing them in the solution for 24 h and withdrawing at a speed of 10 mm/min, followed by extensive rinsing with water along the fixed direction (18). Finally, these films were treated at 100˚C for 60 min in a stream of 20% H_2/80% N_2 in order to partially remove organic agents. The films were then stored in a vacuum for 15 days.

$AgNO_3$ and PDDA were purchased from Sinopharm Chemical Reagent Co., Ltd. (Shanghai, China). CTAB (99%) and mercaptoundecanoic acid were obtained from Sigma-Aldrich; Merck KGaA (Darmstadt, Germany). All other reagents were from Sigma-Aldrich; Merck KGaA and were distributed by Nanjing KeyGen Biotech Co., Ltd. (Nanjing, China). Ultrapure deionized water (Barnstead Nanopure H_2O purification system; Thermo Fisher Scientific, Inc., Waltham, MA, USA) was used throughout the experiments. C225 was purchased from Merck KGaA.

Cell culture. The human nasopharyngeal carcinoma CNE cells, originally isolated from a 58-year-old patient with nasopharyngeal carcinoma, were purchased from Procell Life Science and Technology Co., Ltd. (Wuhan, China; cat. no. CL-0063). The cells were cultured in a humidified atmosphere at 37˚C containing 5% CO_2 in RPMI 1640 medium (Gibco; Thermo Fisher Scientific, Inc.) supplemented with heat-inactivated foetal bovine serum (15% by volume, Bovogen Biologicals Pty Ltd., Melbourne, Australia), penicillin G (50 U/ml) and streptomycin (50 μg/ml). The cell line was maintained in the exponential growth phase and the medium was replaced with fresh medium every 2-3 days.

Enzyme-linked immunosorbent assay (ELISA). A double-antibody sandwich was used to quantify the level of C225 in the Ag/C225 nanocomposites. The CNEs were seeded in a 96-well plate in 300 μl medium at an average density ($1x10^4$/ml) and were grown for 2 days, followed by washing three times with PBS, drying and fixing in 0.125% pentyl glycol for 30 min at 4˚C. The cells in the wells were blocked with 1% BSA (Nanjing KeyGen Biotech Co., Ltd.) at 37˚C for 1 h and washed twice. C225 and Ag/C225 were serially diluted (final concentrations: 72.5, 125, 250 and 500 μg/ml), with six replicates per dilution. Horseradish peroxidase (HRP) goat-anti-mouse IgG (sc-2005, 1:2,000; Santa Cruz Biotechnology, Inc., Dallas, TX, USA) for 2 h at 25˚C and substrate working solution were then added. The absorbance was measured at 450 nm using a microplate spectrophotometer (SpectraMax; Molecular Devices LLC, Sunnyvale, CA, USA).

3-(4,5-dimethylthiazol-2-yl)-2,5-diphenyltetrazolium bromide (MTT) assay of cell proliferation. To examine the cytotoxicity of Fe_3O_4/Ag/C225, the cells were seeded in 96-well plates at a density of $2.5x10^4$ cells/well and allowed to adhere for 24 h at 37˚C. The cells were then cultured in the presence of Fe_3O_4/Ag/C225 (final concentrations: 0.083, 0.166, 0.332, 0.664, 1.328, 2.656, 5.313, 10.63, 21.250 and 42.500 μg/ml) for 48 h, following which MTT (Sigma; Merck KGaA) was added to each well for 4 h at 37˚C. Dimethylsulphoxide (Sigma; Merck KGaA) was then added to each well to dissolve the dark blue crystal product. The absorbance was measured at a wavelength of 488 nm using a microplate reader (Bio-Rad Laboratories, Inc., Hercules, CA, USA).

Irradiation conditions. The cell culture plates and 5-cm thick water tanks were set below a PRIMUS type Siemens linear accelerator (Siemen AG, Munich, Germany). The source

target distance was 100 cm, with a 10x10 cm portal to 6MV X-ray irradiation (dose rate 200 cGy/min). According to the experimental requirements of different doses of irradiation, the irradiated cells were cultured at 37˚C and 5% CO_2 in a humidified incubator.

Analysis of apoptosis. The cells ($5x10^5$) were harvested, washed with PBS and resuspended in binding buffer (Nanjing KeyGen Biotech Co., Ltd.), followed by mixing with Annexin V-FITC and propidium iodide (Nanjing KeyGen Biotech Co., Ltd). The cells were analysed using a BD FACSCalibur flow cytometer provided with CellQuest software (version 5.1; BD Biosciences, Franklin Lakes, NJ, USA). Every experiment was repeated three times.

Cell cycle analysis. The cells ($1x10^6$) were harvested, washed with PBS and fixed in 70% ethanol. The fixed cells were then washed with PBS and resuspended in RNaseA (Nanjing KeyGen Biotech Co., Ltd.), followed by incubation at 37˚C for 30 min. The cells were stained with PI solution (Nanjing KeyGen Biotech Co., Ltd) and analysed using a BD FACSCalibur flow cytometer provided with CellQuest software (BD Biosciences). Every experiment was repeated three times.

Clonogenic assays. The exponentially growing cells were irradiated using an X-ray source at doses of 0, 2, 4, 6 or 8 Gy at room temperature, and then incubated in the presence or absence of Ag/C225 for 24 h at 37˚C. Following incubation, the cells were washed in PBS and trypsinized. The cells were then seeded into a 24-well plate with 5 ml medium at a density of 200 cells/well. Colonies were grown for 10 days. The plates were then washed in PBS and colonies were fixed with 95% ethanol. Staining was performed with 0.1% crystal violet solution. Colonies of >50 cells were counted under an inverted microscope for calculating the surviving fraction. Six parallel samples were scored for each treatment condition.

Western blot analysis. Proteins were extracted with cell lysis buffer (Nanjing KeyGen Biotech Co., Ltd) and quantified via A280 absorption using a NanoDrop 2000C (Thermo Fisher Scientific, Inc.). Equal quantities of proteins (100 μg/lane) were separated on 4-12% NuPAGE Novex Bis-Tris Mini Gels (Invitrogen; Thermo Fisher Scientific, Inc.) and the separated proteins were transferred onto Immobilon-P PVDF membranes (Invitrogen; Thermo Fisher Scientific, Inc.). The membranes were blotted using primary antibodies directed against Ku-80 (rabbit polyclonal IgG, ABP51684, 1:500; Abbkine Scientific Co., Ltd., Wuhan, China), Ku-70 (rabbit polyclonal IgG, sc-9033; 1:300; Santa Cruz Biotechnology, Inc.), Rad51 (rabbit polyclonal IgG, sc-8349, 1:400, Santa Cruz Biotechnology, Inc.) and β-actin (mouse monoclonal IgG, A1978, 1:1000, Sigma-Aldrich; Merck KGaA). Following incubation with the appropriate anti-rabbit (sc-2004) or anti-mouse (Sc-2005) HRP-conjugated secondary antibody (1:10,000; Santa Cruz Biotechnology, Inc.), the immunoreactive bands were visualized using chemiluminescence reagents and exposed to X-ray film. The protein expression of β-actin was used as a normalization control for protein loading.

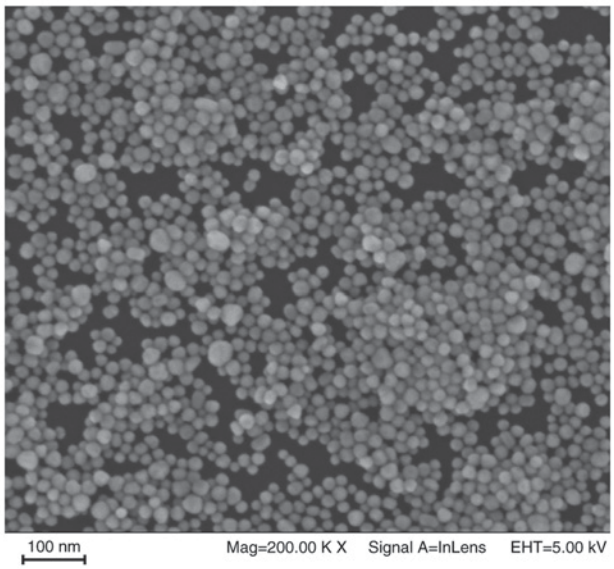

Figure 1. Transmission electron microscope image of AgNPs indicating suitable dispersal and uniformity. The majority of the AgNps were spherical or almost spherical. AgNPs, silver nanoparticles.

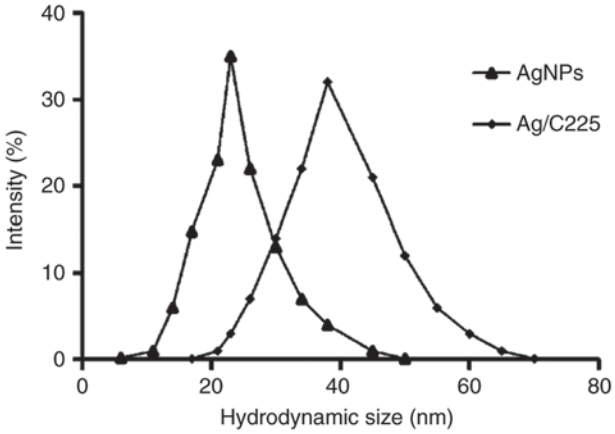

Figure 2. Hydrodynamic size distribution of AgNPs and Ag/C225 nanocomposites were assessed by dynamic light scattering. AgNPs, silver nanoparticles.

Statistical analysis. Data are expressed as the mean ± standard deviation. SPSS version 19 (IBM SPSS, Armonk, NY, USA) statistical software was used to perform one-way analysis of variance, followed by an SNK test. $P<0.05$ was considered to indicate a statistically difference.

Results

Characteristics of AgNPs and Ag/C225 nanocomposites. The morphology of the AgNPs, determined using TEM, is shown in Fig. 1. The majority of nanoparticles were spherical or almost spherical, with sizes ranging between 15 and 45 nm. The ultraviolet spectra of the AgNPs is shown in Fig. 2, indicating that the absorption peak of Ag at 423 nm gradually increased following binding to C225, and was red shifted from 21 to 42 nm.

Activity of the anti-EGFR antibody C225 is preserved in Ag/C225. In order to determine whether the anti-EGFR

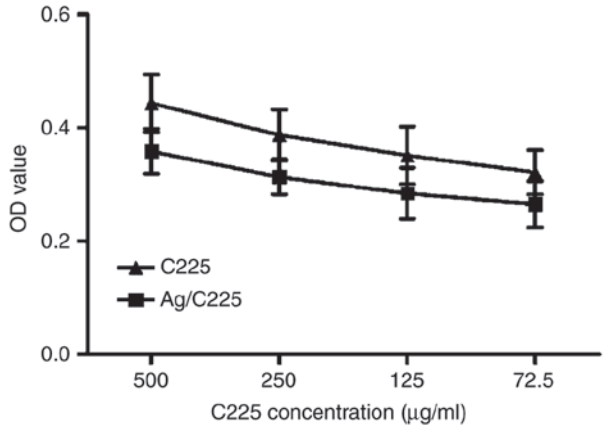

Figure 3. Activity of anti-epidermal growth factor receptor antibody, C225, is preserved in the context of Ag nanoparticles. The average preserved activity was 81.18±4.53%. Data are presented as the mean ± standard deviation (n=3). Ag, silver; OD, optical density.

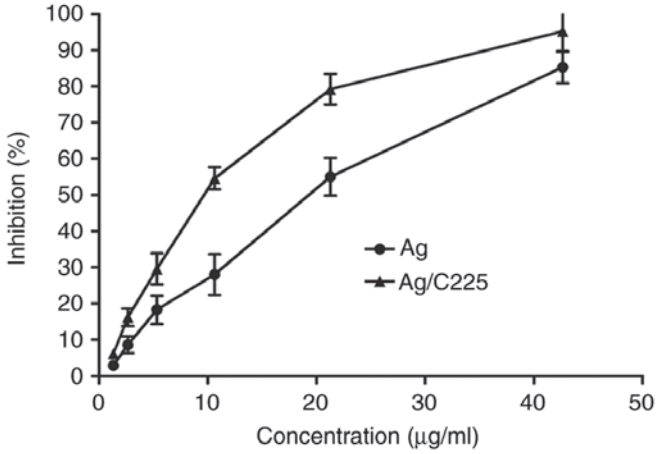

Figure 4. Effect of Ag/C225 on CNE cell proliferation, measured using a 3-(4,5-dimethylthiazol-2-yl)-2,5-diphenyltetrazolium bromide assay. Data are presented as the mean ± standard deviation (n=3). Ag, silver; AgNPs, silver nanoparticles.

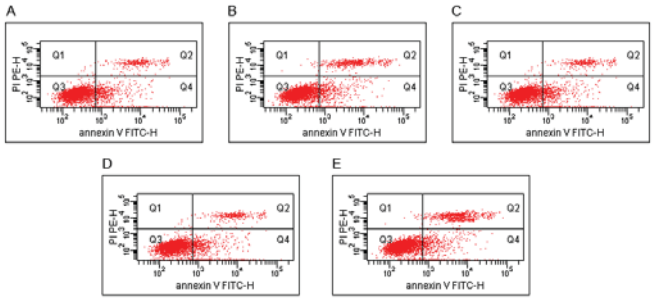

Figure 5. Flow cytometric analysis of apoptosis in nasopharyngeal carcinoma CNE cells. Flow cytometry results of (A) negative control, (B) silver nanoparticles at 1/5 the IC_{50} value, (C) silver nanoparticles at 1/10 the IC_{50} value, (D) silver/C225 nanoparticles at 1/5 the IC_{50} value and (E) silver/C225 nanoparticles at 1/10 the IC_{50} value. Q1, dead cells; Q2, late apoptosis; Q3, living cells; Q4, early apoptosis.

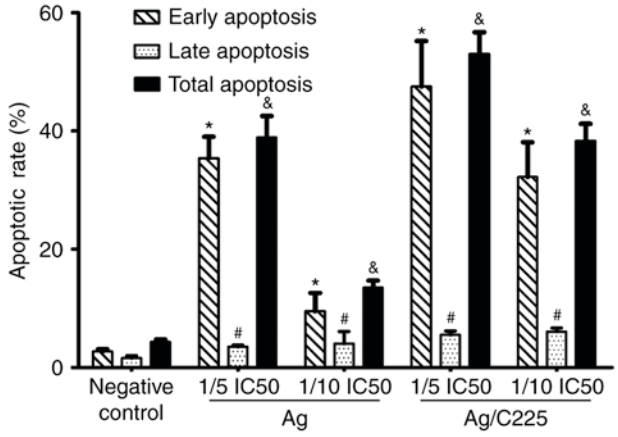

Figure 6. Histogram of the results of flow cytometry showing the effects of AgNPs and Ag/C225 on CNE cell apoptosis. Ag, silver; AgNPs, silver nanoparticles. *P<0.05, vs. negative control in early apoptosis; #P<0.05, vs. negative control in late apoptosis; &P<0.05, vs. negative control in total apoptosis.

antibody C225 retained its activity in the Ag/C225 nanocomposites, ELISA was performed. This revealed that the average preserved activity was 82.17±5.19% [optical density $(OD)_{g/C225}/OD_{C225}$]. The level of preserved activity was highest when the antibody concentration decreased. Specifically, the activity of Ag/C225 at an absolute C225 concentration of 500 μg/ml was 81.18±4.53%, but was 82.17±5.19% when the C225 concentration was 72.5 μg/ml. Therefore, the anti-EGFR antibody activity was retained in the Ag/C225 nanocomposite (Fig. 3).

Ag/C225 causes irreversible growth inhibition. The antiproliferative effect of various concentrations of Ag/C225 on CNE cells is shown in Fig. 4. The results of the MTT assays showed that Ag/C225 inhibited cell growth in a concentration-dependent manner, with half maximal inhibitory concentration (IC_{50}) values of 12.09±1.14 and 9.09±3.47 μg/ml for Ag and Ag/C225 exposure, respectively (P<0.05).

Following irradiation, the Annexin V/PI assay revealed marked induction of apoptosis following treatment with 1.818 μg/ml (1/5 of the IC_{50} value) Ag/C225. The percentage cell death was lower with either Ag/C225 or AgNPs at 1/10 of the IC_{50}. In the control, the fraction of apoptotic cells was 4.31±0.40%. The apoptotic rates of the Ag (1/10 IC_{50}) and (1/5 IC_{50}) treated-groups were 13.53±1.24 and 38.93±3.62%, respectively, whereas the apoptotic rates in the Ag/C225 (1/10 IC_{50}) and (1/5 IC_{50}) treated-groups were 38.36±2.91 and 53.03±3.70%, respectively (Figs. 5 and 6).

Ag/C225 enhances the cytotoxicity induced by X-ray irradiation. The effects of Ag/C225 on the cytotoxic effect of X-ray irradiation in CNE cells were investigated by monitoring cell survival using a clonogenic assay (Fig. 7). The cells were irradiated with different X-ray doses, and then incubated with 2.418 μg/ml Ag and 1.818 μg/ml Ag/C225 (1/5 the IC_{50} value) for 24 h. These concentrations of Ag and Ag/C225 were not cytotoxic alone at the exposure duration used (data not shown). Cell survival curves were plotted with a single-hit multitarget model in order to detect differences between treatment conditions. The parameter D_0 was used to characterize the radiosensitivity in the linear (high-dose) region, and the value of parameter Dq indicated the ability of the cells to repair

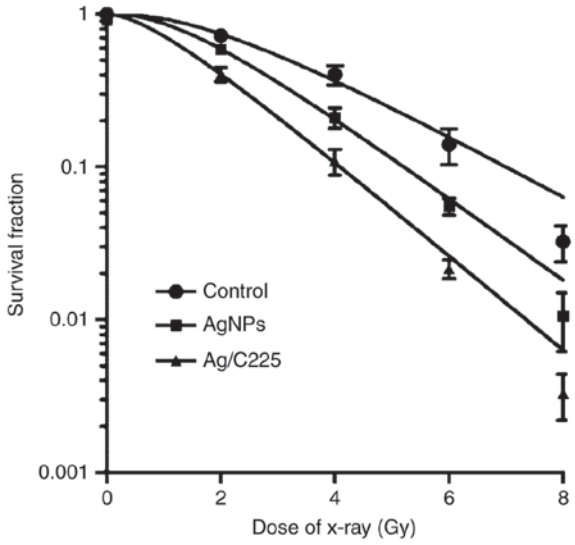

Figure 7. Ag/C225 enhances the cytotoxicity of X-ray irradiation in CNE cells. Cell survival was measured using a clonogenic assay. AgNPs, silver nanoparticles.

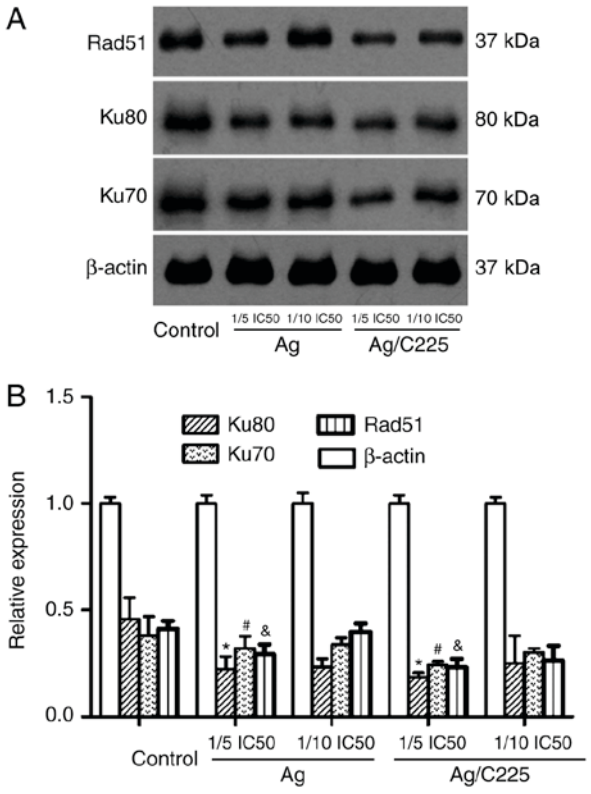

Figure 8. Expression of Ku-70, Ku-80 and Rad51 in CNEs treated with Ag nanoparticles, Ag/C225 and X-ray irradiation (A) Western blot analysis from three independent experiments. (B) Quantification of the western blot analysis results. Ag, silver; IC_{50}, half maximal inhibitory concentration. $^{*}P<0.05$ vs. negative control in Ku-80; $^{\#}P<0.05$ vs. negative control in Ku-70; $^{\&}P<0.05$ vs. negative control in Rad51.

potentially lethal damage in the shoulder (low-dose) region. In the CNE cells, which were irradiated but not treated with NPs, the D_0 and Dq values were 2.145±0.037 and 3.648±0.121 Gy, respectively. For the cells irradiated and treated with Ag and Ag/C225, the values were 1.610±0.012 Gy (Ag for D_0) and 1.405±0.033 Gy (Ag/C225 for D_0) and 2.612±0.014 Gy (Ag for Dq) and 1.234±0.041 Gy (Ag/C225 for Dq), respectively. Therefore, Ag/C225 potentiated the cytotoxicity of X-rays in the CNE cells, compared with exposure to Ag alone, by ~1.142-fold ($D0_{Ag}$ /$D0_{Ag/C225}$). This effect was observed at 1.818 μg/ml Ag/C225 ($P<0.05$). Ag/C225 enhanced the cytotoxic effect of X-rays on the CNE cells by ~1.527-fold ($D0_{control}$/$D0_{Ag/C225}$).

Signalling molecules associated with mitosis arrest. As shown in Fig. 8, Ag or Ag/C225 (at 1/5 the IC_{50} value) downregulated the expression levels of Rad51, Ku-80 and Ku-70. These changes were most marked at 4 h post-treatment with Ag or Ag/C225.

Discussion

Radiation therapy is the front line treatment for ~70% of patients with head and neck malignant tumours (18). However, the efficacy of this treatment modality is compromised due to the need to balance efficacy with unwanted side effects in normal tissues. This has prompted investigations to identify radiosensitizing agents, although clinically effective compounds of this type are difficult to identify (19). Novel *in vivo* tumour imaging agents are also required, as current radionuclide imaging methods have low sensitivity and spatial resolution, and are not without safety issues (20,21).

In the present study, a novel multi-functional composite nanoparticle, Ag/C225, was synthesized, which showed potential for use as a cancer theranostic agent. Unconjugated AgNPs can enhance the inhibitory effect of radiation on tumour cells, and exhibit radiosensitizing effects (22). C225 is an anti-EGFR monoclonal antibody, which has been used clinically to inhibit tumour cell growth; it also exhibits radiosensitizing properties. As the expression of EGFR is high in the majority of solid tumours, the present study hypothesized that the high-affinity C225 antibody in the context of an Ag/C225 formulation may be an effective imaging tracer *in vivo* and *in vitro*. The results of the present study indicated that the activity of C225 was preserved in Ag/C225 NPs, and that it exerted antiproliferative effects in a human CNE cell line.

The Ku heterodimer (composed of Ku-70 and Ku-80) contributes to genomic integrity through its ability to bind DNA double-strand breaks and facilitate repair through the non-homologous end-joining pathway (23,24). In the present study, it was found that Ku-70, Ku-80 and Rad51 were downregulated by AgNPs, and this was more marked upon Ag/C225 treatment.

Ag/C225 was an effective radiosensitizer, suggesting that further pre-clinical and clinical trials with this compound are warranted. Although the molecular mechanism by which Ag/C225 exerts its radiosensitization remains to be elucidated, the present study observed the downregulation of several DNA damage/repair proteins. Therefore, it was hypothesized that Ag/C225 compromises the ability of cells to repair double strand breaks induced by X-ray irradiation, leading to increased tumour cell death.

In conclusion, the results of the present study demonstrated that the multifunctional Ag/C225 nanocomposite was a promising radiosensitizing agent. Future investigations aim to focus

on the molecular mechanisms underlying the effects of this compound, and on defining additional tumour types that may respond well to this agent.

Acknowledgements

The present study was supported by a grant from the National Natural Science Foundation of China (grant no. 81301971).

References

1. Elnaggar YS: Multifaceted applications of bile salts in pharmacy: An emphasis on nanomedicine. Int J Nanomedicine 10: 3955-3971, 2015.
2. Kim SS, Harford JB, Pirollo KF and Chang EH: Effective treatment of glioblastoma requires crossing the blood-brain barrier and targeting tumors including cancer stem cells: The promise of nanomedicine. Biochem Biophys Res Commun 468: 485-489, 2015.
3. Ishihara M, Nguyen VQ, Mori Y, Nakamura S and Hattori H: Adsorption of silver nanoparticles onto different surface structures of chitin/chitosan and correlations with antimicrobial activities. Int J Mol Sci 16: 13973-13988, 2015.
4. Saravanakumar G, Kim K, Park JH, Rhee K and Kwon IC: Current status of nanoparticle-based imaging agents for early diagnosis of cancer and atherosclerosis. J Biomed Nanotechnol 5: 20-35, 2009.
5. Verma A, Uzun O, Hu Y, Hu Y, Han HS, Watson N, Chen S, Irvine DJ and Stellacci F: Surface-structure-regulated cell-membrane penetration by monolayer-protected nanoparticles. Nat Mater 7: 588-595, 2008.
6. Cedervall T, Lynch I, Lindman S, Berggård T, Thulin E, Nilsson H, Dawson KA and Linse S: Understanding the nanoparticle-protein corona using methods to quantify exchange rates and affinities of proteins for nanoparticles. Proc Natl Acad Sci USA 104: 2050-2055, 2007.
7. Chithrani BD, Ghazani AA and Chan WC: Determining the size and shape dependence of gold nanoparticle uptake into mammalian cells. Nano Lett 6: 662-668, 2006.
8. Buckle T, Chin PT and van Leeuwen FW: (Non-targeted) radioactive/fluorescent nanoparticles and their potential in combined pre- and intraoperative imaging during sentinel lymph node resection. Nanotechnology 21: 482001, 2010.
9. Bailet JW, Mark RJ, Abemayor E, Lee SP, Tran LM, Juillard G and Ward PH: Nasopharyngeal carcinoma: Treatment results with primary radiation therapy. Laryngoscope 102: 965-972, 1992.
10. Fandi A and Cvitkovic E: Biology and treatment of nasopharyngeal cancer. Curr Opin Oncol 7: 255-263, 1995.
11. Vivanco I and Sawyers CL: The phosphatidylinositol 3-Kinase AKT pathway in human cancer. Nat Rev Cancer 2: 489-501, 2002.
12. Mendelsohn J: Targeting the epidermal growth factor receptor for cancer therapy. J Clin Oncol 20 (18 Suppl): 1S-13S, 2002.
13. Gril B, Palmieri D, Bronder JL, Herring JM, Vega-Valle E, Feigenbaum L, Liewehr DJ, Steinberg SM, Merino MJ, Rubin SD and Steeg PS: Effect of lapatinib on the outgrowth of metastatic breast cancer cells to the brain. J Natl Cancer Inst 100: 1092-1103, 2008.
14. Unruh A, Ressel A, Mohamed HG, Johnson RS, Nadrowitz R, Richter E, Katschinski DM and Wenger RH: The hypoxia-inducible factor-1 alpha is a negative factor for tumor therapy. Oncogene 22: 3213-3220, 2003.
15. Le QT DenkoNC and Giaccia AJ: Hypoxic gene expression and metastasis. Cancer Metastasis Rev 23: 293-310, 2004.
16. Bonner JA, Harari PM, Giralt J, Azarnia N, Shin DM, Cohen RB, Jones CU, Sur R, Raben D, Jassem J, *et al*: Radiotherapy plus cetuximab for squamous-cell carcinoma of the head and neck. N Engl J Med 354: 567-578, 2006.
17. Xu R, Ma J, Sun X, Chen Z, Jiang X, Guo Z, Huang L, Li Y, Wang M, Wang C, *et al*: Ag nanoparticles sensitize IR-induced killing of cancer cells. Cell Res 19: 1031-1034, 2009.
18. Yang Y, Shi J, Tanaka T and Nogami M: Self-assembled silver nanochains for surface-enhanced Raman scattering. Langmuir 23: 12042-12047, 2007.
19. Livak KJ and Schmittgen TD: Analysis of relative gene expression data using real-time quantitative PCR and the 2(-Delta Delta C(T)) method. Methods 25: 402-408, 2001.
20. Neklasova NY, Zharinov GM and Grebenyuk AN: Modification of radiosensitivity in maignant and normal tissues during radiotherapy of malignant neoplasms. Radiats Biol Radioecol 54: 597-605, 2014 (In Russian).
21. Pelevina II, Aleshchenko AV, Antoshchina MM, Birjukov VA, Reva EV and Minaeva NG: The radiosensitivity change after low-dose irradiation, possible mechanisms and regularities. Radiats Biol Radioecol 55: 57-62, 2015 (In Russian).
22. Zhao D, Sun X, Tong J, Ma J, Bu X, Xu R and Fan R: A novel multifunctional nanocomposite C225-conjugated Fe3O4/Ag enhances the sensitivity of nasopharyngeal carcinoma cells to radiotherapy. Acta Biochim Biophys Sin (Shanghai) 44: 678-684, 2012.
23. Evans-Axelsson S, Vilhelmsson Timmermand O, Welinder C, Borrebaeck CA, Strand SE, Tran TA and Jansson B: Preclinical evaluation of (111)In-DTPA-INCA-X anti-Ku70/Ku80 monoclonal antibody in prostate cancer. Am J Nucl Med Mol Imaging 4: 311-323, 2014.
24. O'Sullivan D, Henry M, Joyce H, Walsh N, Mc Auley E, Dowling P, Swan N, Moriarty M, Barnham P, Clynes M and Larkin A: 7B7: A novel antibody directed against the Ku70/Ku80 heterodimer blocks invasion in pancreatic and lung cancer cells. Tumour Biol 35: 6983-6997, 2014.